Chaos, Solitons and Fractals 140 (2020) 110149

Contents lists available at ScienceDirect

Chaos, Solitons and Fractals

Nonlinear Science, and Nonequilibrium and Complex Phenomena

journal homepage: www.elsevier.com/locate/chaos

Fractional order controllers increase the robustness of closed-loop deep brain stimulation systems

Antonio Coronel-Escamilla[a], Jose Francisco Gomez-Aguilar[b], Ivanka Stamova[c], Fidel Santamaria[a,*]

[a] Department of Biology, University of Texas at San Antonio, San Antonio, TX 78249, USA
[b] National Center for Research and Technological Development, (CENIDET), Morelos, 62490, Mexico
[c] Department of Mathematics, University of Texas at San Antonio, San Antonio, TX 78249, USA

ARTICLE INFO

Article history:
Received 8 April 2020
Revised 7 July 2020
Accepted 23 July 2020

Keywords:
Control theory
Fractional order calculus
Basal ganglia
Motor disorders
Lyapunov-stability

ABSTRACT

We studied the effects of using fractional order proportional, integral, and derivative (PID) controllers in a closed-loop mathematical model of deep brain stimulation. The objective of the controller was to dampen oscillations from a neural network model of Parkinson's disease. We varied intrinsic parameters, such as the gain of the controller, and extrinsic variables, such as the excitability of the network. We found that in most cases, fractional order components increased the robustness of the model multi-fold to changes in the gains of the controller. Similarly, the controller could be set to a fixed set of gains and remain stable to a much larger range, than for the classical PID case, of changes in synaptic weights that otherwise would cause oscillatory activity. The increase in robustness is a consequence of the properties of fractional order derivatives that provide an intrinsic memory trace of past activity, which works as a negative feedback system. Fractional order PID controllers could provide a platform to develop stand-alone closed-loop deep brain stimulation systems.

© 2020 Elsevier Ltd. All rights reserved.

1. Introduction

Deep brain stimulation (DBS) is widely used to treat multiple pathological conditions [11,30,35,43,49]. DBS consists in implanting a multi-contact lead to one or different parts of the brain to deliver brief electrical pulses. Recent evidence shows that closed-loop systems can provide better treatments to pathologies such as Parkinson's disease [29,63]. However, changes in the conditions of the implant or the intrinsic dynamics of the neuronal population can change over time; thus, reducing the effectiveness of the treatment. Therefore, it is important to develop techniques that allow closed-loop systems to be robust to intrinsic changes, such as changes in the conductance of the electrodes; or extrinsic, such as changes in the excitability of the neural network it aims to control [14,21,23,31,47].

Outside the field of DBS there is an emerging field within closed-loop control theory that uses fractional order dynamical components [65]. Fractional order dynamics uses derivatives and integrals with non-integer order [8]. Fractional order models are used to study systems in which the complex interactions of its elements result in no specific time constant dominating the dynamics [6,39,60]. A characteristic of fractional order systems, and in contrast to integer order integro-differential equations, is that they have what is known as an 'intrinsic memory'. The intrinsic memory trace arises from the non-local properties of the fractional order operator. From a control system perspective, the intrinsic memory trace is a negative feedback mechanism that reacts fast to sudden changes while allowing long-term adaptation [7,36,81]. Moreover, there is increasing evidence that fractional order closed-loop systems are ideal to control complex processes and machinery [4,19,69,74]. Because of these properties, we hypothesized that fractional order controllers could provide a flexible and robust framework to implement closed-loop DBS systems.

In this work, we implemented a proportional, integral, and differential (PID) controller with fractional orders to regulate the firing rate activity in a mathematical model of DBS of Parkinson's disease. A fractional PID controller is the generalization of the classical PID controller, but involving fractional order integro-differential elements [20]. Several studies have shown the effectiveness of closed-loop controllers applied to biomedical problems, from drug administration treatments [5,52,53,67,68], to dynamical disorders of the brain related to abnormal activity, such as epilepsy and

* Corresponding author.
E-mail address: fidel.santamaria@utsa.edu (F. Santamaria).

https://doi.org/10.1016/j.chaos.2020.110149
0960-0779/© 2020 Elsevier Ltd. All rights reserved.

Parkinson's [26,28,48,62,73]. The use of fractional order PID controllers has been shown to provide improved performance than in the classical cases [27,69]. In this work, we show that the fractional controller dampens the pathological oscillatory behavior over a wider range of synaptic and controller parameters compared to the integer-order controller. Furthermore, we show that the controller is robust to random changes in synaptic parameters, thus allowing the dynamical control of the oscillation under changes in intrinsic conditions. Since the properties of the fractional order controller are independent of the nature of the oscillations we suggest that this approach could be used to implement robust DBS for Parkinson's disease and other pathological conditions.

The manuscript is organized as follows. Section 2 provides the fractional order calculus definitions used in this work. Section 3 describes the mathematical model and the fractional order PID controller design. Section 4 presents a Lyapunov-based stability analysis of the mathematical model with the fractional PID controller. Section 5 shows the numerical method used to compute the fractional integral and fractional derivative. Section 6 presents the results obtained in this work. Finally, Section 7 presents a discussion and point to potential avenues for implementation.

2. Fractional calculus definitions

There are multiple definitions of fractional order derivative and integrals. Some of them only apply to one but not the other. Because we required to compute derivatives and integrals in this work we decided to use the Riemann-Liouville definition that applies to both operators [9,44].

Let $f:(0,\infty)\to\mathbb{R}$ be a continuous function. Then the integral operator in the Riemann-Liouville sense is defined as follow of order $\alpha>0$, $\alpha\in\mathbb{R}$ is given by [38]

$$ {}_0^{RL}I_t^{\alpha} f(t) = \frac{1}{\Gamma(\alpha)}\frac{d^m}{dt^m}\int_0^t f(\eta)(t-\eta)^{\alpha-1}d\eta, t>0 \tag{1}$$

where $\Gamma(\cdot)$ is the Gamma function. If $\alpha\in\mathbb{Z}$, then the above integral is defined as in the classical case.

Let $\beta>0$ and $m=[\beta]+1$. Then the Riemann-Liouville fractional derivative of order β is

$$ {}_0^{RL}D_t^{\beta} f(t) = \frac{1}{\Gamma(m-\beta)}\frac{d^m}{dt^m}\int_0^t f(\eta)(t-\eta)^{m-\beta-1}d\eta, t>0 \tag{2}$$

if $\beta\in\mathbb{Z}$, then the above derivative is defined as in the classical case. The Gamma function is defined as

$$\Gamma(z)=\int_0^{\infty} t^{z-1}\exp(-t)dt \tag{3}$$

3. Mathematical model of Parkinson's disease in the basal ganglia

Parkinson's disease is characterized by difficulty in the initiation of movement believed to be caused by abnormal firing rate oscillations in the beta range, ~12.5 Hz to 30 Hz, in the activity of the neurons within the basal ganglia [12,33,51,56,64]. DBS consists in implanting a multi-contact lead, in either the ventral thalamus, the internal segment of the globus pallidus (GP), or the subthalamic nucleus (STN) and applying short-duration stimuli at a constant high frequency [25,50]. The parameters of the stimulation are usually fixed with only sporadic manual adjustments [2,10,41,42,58,64]. We based our study on a previously published model to study Parkinson's disease [33,54,56]. The model implements a circuit of the basal ganglia with connections between the GP, STN, Striatum, and the cortex, Eq. (4) and Fig. 1. Let

Table 1
Network parameters.

Parameter	Value	Description
δ_{sg}	6 ms	Delay STN→GP
δ_{gs}	6 ms	Delay GP→STN
δ_{gg}	4 ms	Delay GP→GP
τ_s	6 ms	Reaction time STN
τ_g	14 ms	Reaction time GP
M_s	300 spk/s	STN maximum firing rate
B_s	17 spk/s	STN resting firing rate
M_g	400 spk/s	GP maximum firing rate
B_g	75 spk/s	GP resting firing rate
ν_s	27 spk/s	Cortical input to STN
ν_g	2 spk/s	Striatal input to GP

Table 2
Synaptic weights in healthy and disease states.

Parameter	Healthy	Disease	Connections
ω_{gs}	1.12	10.7	GP→STN
ω_{sg}	19.0	20.0	STN→GP
ω_{gg}	6.60	12.3	GP→GP
ω_{cs}	2.42	9.2	Cortex→STN
ω_{xg}	15.1	139.4	Striatum→GP

$\mathbb{R}_+=[0,\infty)$, then the model is given by

$$\begin{aligned}\tau_s\frac{d}{dt}STN(t) &= -STN(t)+F_s(-\omega_{gs}GP(t-\delta_{gs})+\omega_{cs}\nu_s+u(t))\\ \tau_g\frac{d}{dt}GP(t) &= -GP(t)+F_g(-\omega_{sg}STN(t-\delta_{sg})-\omega_{gg}GP(t-\delta_{gg})\\ &\quad+\omega_{gg}\nu_g)\end{aligned} \tag{4}$$

where $STN(t)$ and $GP(t)$ are the firing rate of the STN and GP, respectively. The functions F_s and F_g are

$$\begin{aligned}F_s &= \frac{M_s}{1+\left(\frac{M_s-B_s}{B_s}\right)e^{\left(\frac{-4x}{M_s}\right)}}\\ F_g &= \frac{M_g}{1+\left(\frac{M_g-B_g}{B_g}\right)e^{\left(\frac{-4x}{M_g}\right)}}\end{aligned} \tag{5}$$

where x is the input as shown in Eq. (4). The rest of the parameters are described in Table 1.

The function $u(t)$ represents the input of the controller. In the classical case, we use a PID controller given as

$$u(t)=K_P e(t)+K_I\int_0^t e(\tau)d\tau+K_D\frac{d}{dt}e(t) \tag{6}$$

where K_P, K_I, and K_D are the gains of the proportional, integral, and differential components, respectively. The error function is defined as

$$e(t)=STN_d-LFP(t) \tag{7}$$

where STN_d is the target firing rate for the STN. The function LFP represents the local field potential in the GP, which receives inputs from the STN and Striatum. Since in the model, the striatum provides a constant input then we simplify this to be

$$LFP(t)=\omega_{sg}STN(t-\delta_{sg}) \tag{8}$$

which is the weighted delayed activity of the STN (see Eq. (4)). The output of the controller is then injected into the STN.

Parkinson's disease condition requires changes in the synaptic weights between the STN and the GP, the striatum and the GP, and the cortex and the STN [33], see Table 2.

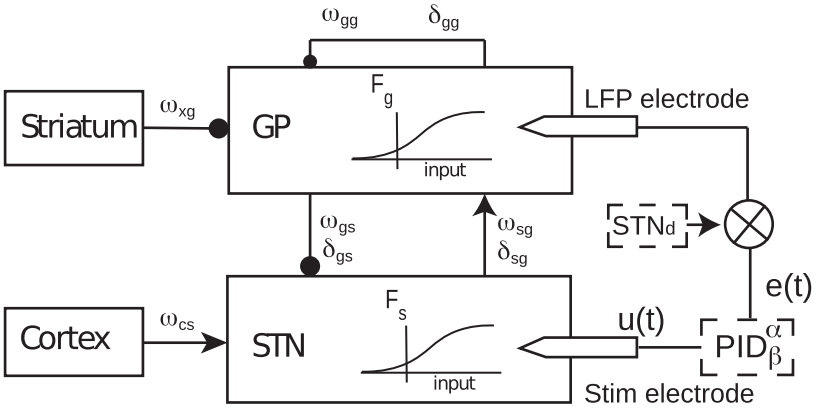

Fig. 1. Basal ganglia model and a closed-loop control system. The firing rate network model is composed of the striatum, cortex, Globus Pallidus (GP), and sub-thalamic nucleus (STN). The controller is composed of an electrode that monitors the local field potential (LFP) in GP and a stimulation electrode, u(t), in the SNT. The controller is set to maintain the firing rate of the STN to a set point (STNd), by calculating an error function, e(t). The feedback is calculated using a proportional, integrator, and differential controller with fractional order integration (α) and differentiation (β). The dynamics of the model depend on synaptic weights (ω_{gs}, ω_{sg}, ω_{gg}, ω_{xg}, ω_{cs}) and propagation delays (δ_{gg}, δ_{gs}, δ_{sg}). Synapses marked with $\rightarrow$ are excitatory and with $\bullet$ are inhibitory. See text for details.

In this work we generalize the classical PID controller to a fractional order controller which is characterized by the order α, for the integral; and β, for the differential components, then Eq. (6) results as

$$u(t) = K_P e(t) + K_{I_0}^{RL} I_t^{\alpha} e(t) + K_{D_0}^{RL} D_t^{\beta} e(t) \tag{9}$$

where operators ${}_0^{RL}I_t^{\alpha}$ and ${}_0^{RL}D_t^{\beta}$represent the fractional integral and the fractional derivative in the Riemann-Liouville sense, respectively. The exponents α and β are the order of the integral and derivative, respectively [59,60]. If $\alpha = \beta = 1$ the controller is identical to Eq. (6). Finally, the controlled system given in Eq. (4) with the fractional PID controller given in Eq. (9) takes the form

$$\begin{aligned} \tau_s \frac{d}{dt} STN(t) &= -STN(t) + F_s\Big(-\omega_{gs} GP(t-\delta_{gs}) + \omega_{cs} v_s + K_P e(t) + K_{I_0}^{RL} I_t^{\alpha} e(t) + K_{D_0}^{RL} D_t^{\beta} e(t).\Big) \\ \tau_g \frac{d}{dt} GP(t) &= -GP(t) + F_g(-\omega_{sg} STN(t-\delta_{sg}) - \omega_{gg} GP(t-\delta_{gg}) + \omega_{gg} v_g) \end{aligned} \tag{10}$$

Based on the basic properties of fractional calculus [60], the fractional integral and derivative of the error result as

$$\begin{aligned} {}_0^{RL}I_t^{\alpha} e(t) &= \frac{STN_d t^{\alpha}}{\Gamma(\alpha)\alpha} - \frac{1}{\Gamma(\alpha)} \frac{d}{dt} \int_a^t e(\eta)(t-\eta)^{\alpha-1} d\eta \\ {}_0^{RL}D_t^{\beta} e(t) &= \frac{STN_d}{\Gamma(1-\beta)t^{\beta}} - \frac{1}{\Gamma(m-\beta)} \frac{d}{dt} \int_a^t \frac{e(\eta)}{(t-\eta)^{\beta}} d\eta \end{aligned} \tag{11}$$

4. Lyapunov-based stability analysis

In this section, we will present a Lyapunov-based stability analysis of the system given in Eq. (4) with the fractional PID controller given in Eq. (9).

Denote by $\delta = \max\{\delta_{gs}, \delta_{sg}, \delta_{gg}\}$, and let for $t \geq 0$, $x_t \in C[[-\delta, 0], \mathbb{R}]$ is defined by $x_t(\gamma) = x(t+\gamma)$, $-\delta \leq \gamma \leq 0$. Let

$$\begin{aligned} f(t, \varphi_t, \phi_t) &= -\varphi(t) + F_s\Big(-\omega_{gs}\phi_t + \omega_{cs} v_s + K_P e(t) + K_{I_0}^{RL} I_t^{\alpha} e(t) + K_{D_0}^{RL} D_t^{\beta} e(t)\Big) \\ g(t, \varphi_t, \phi_t) &= -\phi(t) + F_g(\omega_{sg}\varphi_t - \omega_{gg}\phi_s - \omega_{xg} v_g) \end{aligned} \tag{12}$$

and $(STN(t), GP(t))$, be a solution of (7) with initial data

$$\begin{cases} STN(t; 0, \varphi_0, \phi_0) = \varphi_0(t), & -\delta \leq t \leq 0 \\ GP(t; 0, \varphi_0, \phi_0) = \phi_0(t), & -\delta \leq t \leq 0 \end{cases} \tag{13}$$

where φ_0, ϕ_0 are continuous functions on $[-\delta, 0]$.

Let denote the GP_d the state corresponding to STN_d. Consider the Lyapunov-like functions

$$V(t, STN, GP) = |STN - STN_d| + |GP - GP_d| \tag{14}$$

We will evaluate the derivative of the continuous function V with respect to system given in Eq. (4) defined as

$$D_4^{+} V(t, \varphi(t), \phi(t)) = \lim_{h \to 0^{+}} \sup \frac{1}{\delta} [V(t+h, \varphi(t) + hf(t, \varphi_t, \phi_t), \phi(t) + hg(t, \varphi_t, \phi_t)) - V(t, \varphi(t), \phi(t))] \tag{15}$$

For the sigmoid activation functions F_s and $F_g$there exists positive constants L_s and L_g see [34] such that

$$\begin{aligned} |F_s(x) - F_s(y)| &\leq L_s |x - y| \\ |F_g(x) - F_g(y)| &\leq L_g |x - y| \end{aligned} \tag{16}$$

for all $x, y \in \mathbb{R}$, $x \neq y$ and we also have that $F_g(0) = B_g \geq 0$, $F_s(0) = B_s \geq 0$.

Then for $t \geq 0$,and for any $\varphi \in C[[t-\delta, t], \mathbb{R}]$, $\phi \in C[[t-\delta, t], \mathbb{R}]$ such that $V(t+\gamma, \varphi(t+\gamma), \phi(t+\gamma)) < V(t, \varphi(t), \phi(t))$, $\gamma \in [-\delta, 0)$, we have

$$D_7^+ V(t, \varphi(t), \phi(t)) \leq \left(-\frac{1}{\tau} + A\right) V(t, \varphi(t), \phi(t)) \tag{17}$$

where $-\frac{1}{\tau} = \min\{\frac{1}{\tau_s}, \frac{1}{\tau_g}\}$ and

$$A = \max\left\{\frac{\omega_{gs} L_s}{\tau_s} + \frac{\omega_{gg} L_g}{\tau_g}, \omega_{sg}\left(\frac{1}{\tau_s} L_s\left(K_P + K_I \frac{I_c}{\Gamma(\alpha)} + K_D \frac{D_c}{\Gamma(m-\beta)}\right) + \frac{1}{\tau_g} L_g\right)\right\} \tag{18}$$

where I_c and D_c are constants that will allow to estimate and control the reference gain from the fractional integral and fractional derivative terms.

If $\frac{1}{\tau} \geq A$, then $D_4^+ V(t, \varphi(t), \phi(t)) \leq 0$, and according to the theory of delayed systems [32], the state (STN_d, GP_d) is stable. If, in addition, there is a $c > 0$ such that $\frac{1}{\tau} - A \geq c > 0$, then $D_4^+ V(t, \varphi(t), \phi(t)) \leq -cV(t, \varphi(t), \phi(t))$, which will guarantee the exponential stability. Similar results for fractional order systems are presented in [70–72]. Note that, for such systems the notion of Mittag-Leffler stability generalizes the exponential stability concept.

The Lyapunov-based stability analysis indicates that the behavior of $STN(t)$ and $GP(t)$ could be controlled and synchronized. However, the condition $\frac{1}{\tau} - A \geq c > 0$ is very restrictive. Moreover, to evaluate the effect of adding fractional order integral and derivative elements in the controller and reduce A, numerical simulations for different values of α and β are conducted in the next section.

5. Numerical solution of fractional order derivatives and integrals

While the Riemann-Liouville definition is used for analytical calculus the Grunwald-Letnikov is commonly used for numerical calculus [57,60], this definition is formulated as

$${}_0^{GL}D_t^\theta f(t) = \lim_{h \to 0} \frac{1}{h^\theta} \sum_{j=0}^{t/h} (-1)^j \binom{\theta}{j} f(t - jh) \tag{19}$$

where j is the time increment, ${}_0^{GL}D_t^\theta$ is the fractional operator in the sense of Grunwald-Letnikov, and $\theta \in \mathbb{R}$. For order $\theta < 0$ this is the fractional integral ($\theta = \alpha$), and for $\theta > 0$ is the fractional derivative ($\theta = \beta$). For binomial coefficients calculation, we can use the relation between Euler's Gamma function and factorial, defined as

$$\binom{\theta}{j} = \frac{\Gamma(\theta + 1)}{\Gamma(j+1)\Gamma(\theta - j + 1)} \tag{20}$$

Then, a fractional differential equation expressed as

$${}_0^{GL}D_t^\theta f(t) = g(f(t), t) \tag{21}$$

can be solved numerically as [79]

$$f(t_k) = f(t_{k-1}) h^\theta - \sum_{j=1}^{k} c_j^\theta f\left(t_{k-j}\right) \tag{22}$$

$$c_j^\theta = \left(1 - \frac{1+\theta}{j}\right) c_{j-1}^\theta \tag{23}$$

With $c_0^\theta = 1$, and h is the time step, when θ is negative represents the fractional integral [17,39]. The second part of Eq. (22) is called the intrinsic memory trace. We implemented the entire system in Matlab (Natick, MA). All simulation scripts are available at www.utsa.edu/SantamariaLab and github.com/SantamariaLab.

6. Results

A general challenge in any closed-loop DBS system is to implement algorithms that change the stimulation parameters in response to changes in the conditions of the implant or the activity of the monitored neural network. Here, we take a different strategy by using fractional order controllers. Fractional order controllers provide an intrinsic negative feedback process of previous activity that results in highly flexible modulators of complex systems. To test whether fractional order controllers could be applicable to closed-loop DBS we performed a modeling study of a basal ganglia network in normal and Parkinson's conditions [16]. The normal state of the neural network is when the STN and GP have a stable firing rate (Fig. 2A, $t < 0$). A change in the synaptic parameters (Table 2) results in pathological oscillatory firing rate activity in the beta range (12 Hz) in both areas (Fig. 2A, $t > 0$). We first implemented a proportional controller characterized by the gain K_P, with $K_I = K_D = 0$. We performed a parameter space sweep of the values of K_P to determine the range in which the proportional controller dampened the oscillations. The system was considered under control if the firing rate of the STN was within 10% of the target firing rate (22 Hz) in the last 0.2 s of a 2.5 s long simulation. This resulted in a range of values of $K_P = (15,\ 55)$, which is consistent with a previous modeling report [55]. Outside these values, the controller fails and the activity of the STN oscillates (not shown).

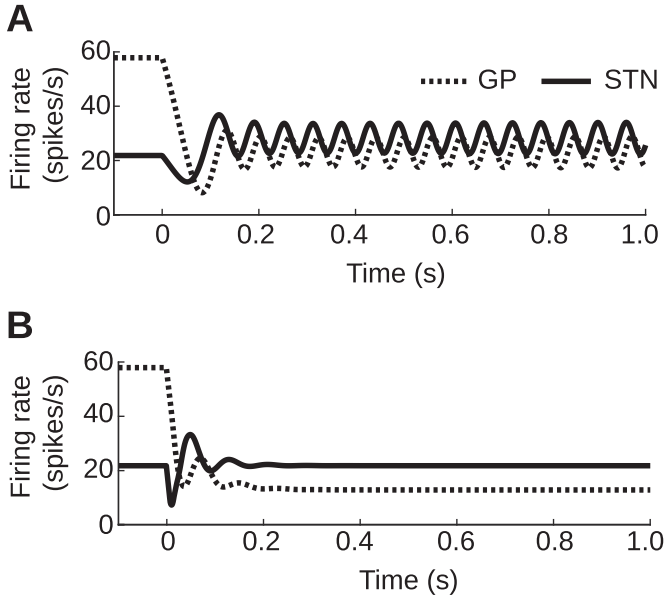

Fig. 2. Modeling Parkinson's disease and its control. **A**) Firing rate versus time of the sub-thalamic nucleus (STN) and Globus Pallidus (GP) before ($t < 0$) and after ($t > 0$) changing synaptic parameters that result in pathological oscillatory behavior, see Table 2. **B**) The same simulation as in B but with the PID controller active all the time set to control the firing rate of the STN. The controller gains were $K_p = 15$, $K_i = 115$, and $K_d = 0.15$.

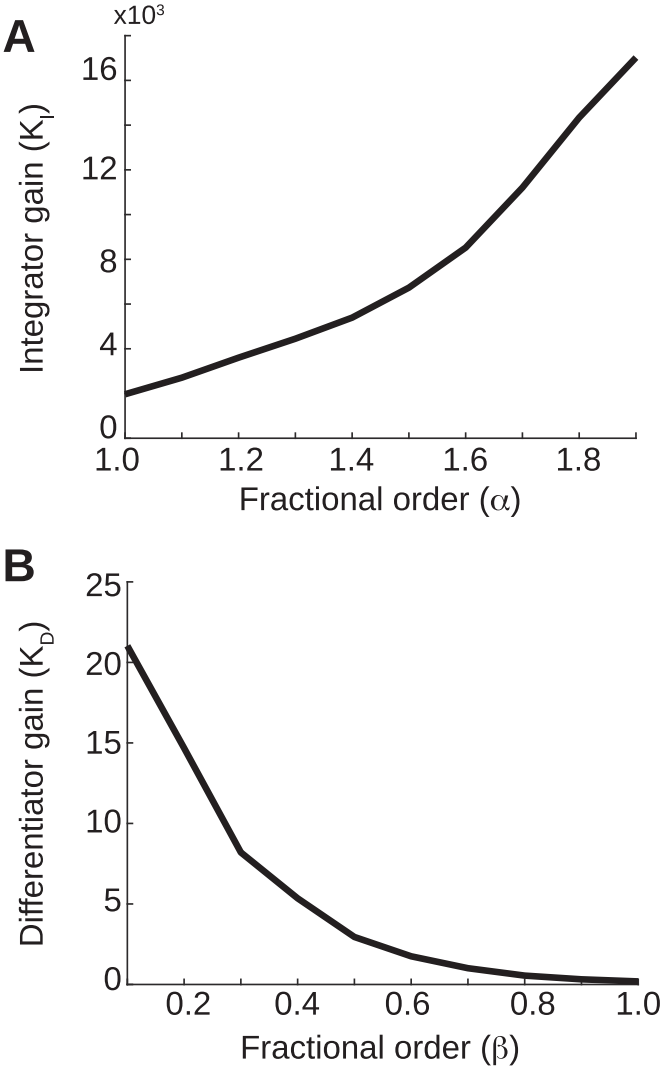

Fig. 3. A fractional order PID results in increase in the range of gains that can be used to control pathological oscillations. **A**) The maximum value of the integral gain (K_i) that could control the oscillations versus the order of the fractional integral (α). $K_p = 15$ and $K_d = 0$. **B**) The maximum value of the derivative gain (K_d) that could control the oscillations versus the order of the fractional derivative (β). $K_p = 15$ and $K_i = 0$.

We then studied the effects of incorporating the integral and derivative elements of the controller $K_I \neq 0$ and $K_D \neq 0$, respectively. As described in Methods, instead of using the classical first order derivative and integral we implemented fractional order integral and derivative operators characterized by their order α and β, respectively. For values of $\alpha = \beta = 1$ ($PID^{\alpha=1}_{\beta=1}$), the controller is identical to the classical integer order PID, Eqs. (6) and (9). For $PID^{\alpha=1}_{\beta=1}$ a parameter sweep of K_I with $K_D = 0$ and $K_P = 15$ resulted in a range of $K_I = (0, 856)$ in which the controller damped the oscillations. A similar analysis by fixing $K_I = 0$ and $K_P = 15$ resulted in a range of $K_D = (0, 0.19)$. To characterize the combined use of the $PID^{\alpha=1}_{\beta=1}$ controller we chose a reference gain ($K_I = 115$, $K_D = 0.15$, $K_P = 15$). This set of gains was able to dampen the oscillatory behavior to the target firing rate in the STN and GP (Fig. 2B). We determined again the ranges of the gains but now fixing either $K_I = 115$ or $K_D = 0.15$. This analysis showed an increase in the range of $K_I = (0,\ 1967)$, while the range for K_D remained unchanged. Thus, a $PID^{\alpha=1}_{\beta=1}$ controller has a narrow value of derivative gains and a large parameter range in the integral component, consistent with the slow nature of the oscillation being controlled.

Once we characterized the $PID^{\alpha=1}_{\beta=1}$controller we investigated the effects on the ranges of K_I and K_D when varying the fractional order of the integral and derivative components, α and β. We first characterized the changes to K_I by keeping $K_D = 0.15$ and $K_P = 15$, and $\beta = 1$. As mentioned before a value of $\alpha = 1$ results in the first integral, which is a measure of the total activity in the system. The second integral provides information on the direction of the accumulation of this activity. Thus, a fractional integral between 1 and 2 provides a mixture of information about the total activity and its overall trajectory as a function of time. Due to these properties, we varied the value of α from 1 to 1.9. This analysis shows that the range of K_I is expanded, going from 0 to 17,000, which is 8.6 times the maximum value than for the $PID^{\alpha=1}_{\beta=1}$ case, Fig. 3A.

Similar to our argument of the fractional integral, a fractional derivative between 0 and 1 provides a mixture of information of past and instantaneous activity. The fractional derivative of a sine is $D^{\beta}\sin(t) = \sin(2\pi ft + \alpha\pi/2)$, this provides a phase advance from the monitored signal that can then be used to predict the behavior of the system. We performed the same analysis as in the fractional integral case while keeping $K_I = 115$ and $\alpha = 1$. Our results show that as the value of β decreases the maximum range of K_D that can control the oscillations expands to $K_D = 22$, an 11-fold increase in the range compared to the $PID^{\alpha=1}_{\beta=1}$ controller, Fig. 3B. The combined analysis of using fractional the $PID^{\alpha>1}_{\beta<1}$ shows a multi-fold increase in the range of operational gains compared to the classical case.

Another form of understanding our results is that the increase in the robustness in the range of gains when using $PID^{\alpha>1}_{\beta<1}$ is due to what is known as the intrinsic memory trace. The intrinsic memory trace, Eq. (21), is a negative feedback function that decays as a power-law in time and is the property that provides the non-locality to the fractional operators. To illustrate the function of the intrinsic memory trace in controlling the system we analyzed two simulations in which all parameters were identical, with $\alpha = 1.5$ and $\beta = 0.5$ and $K_I = 5788$, except for the value of K_D. In one

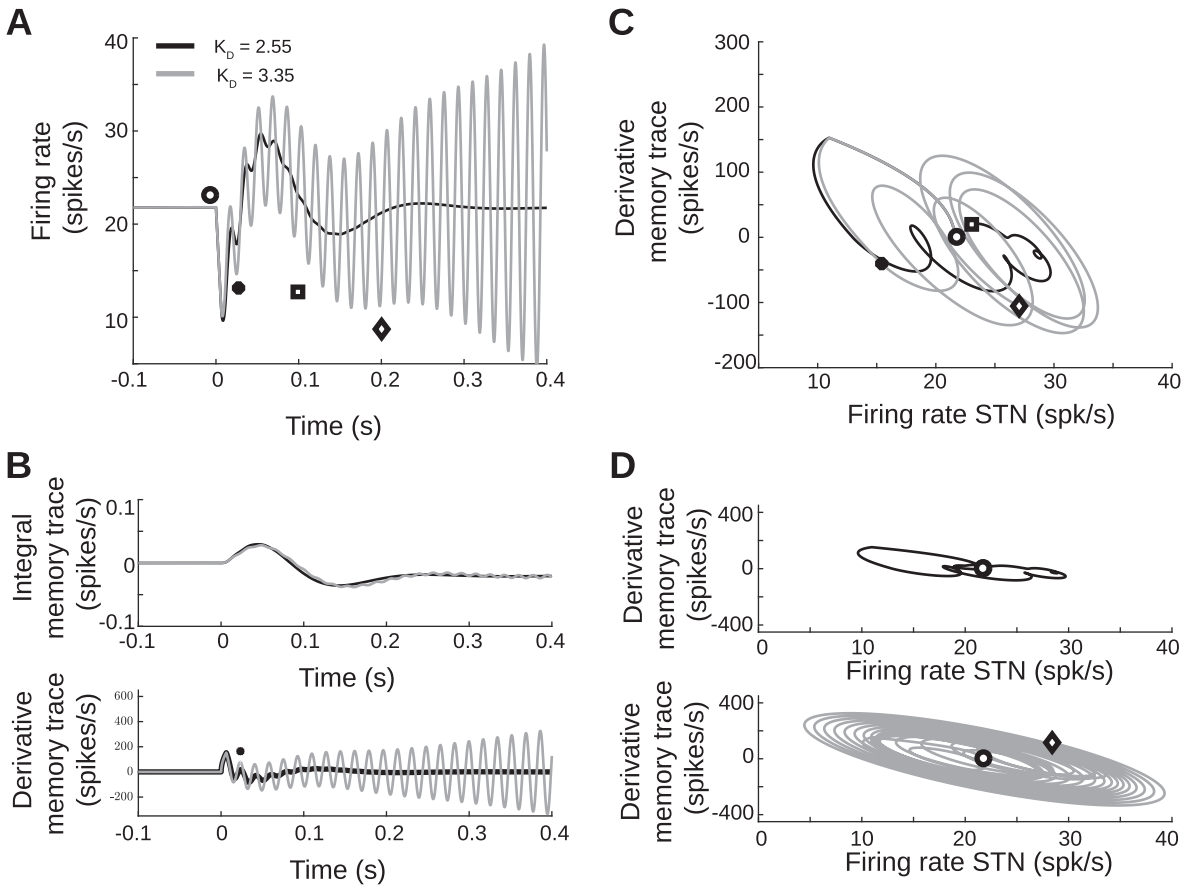

Fig. 4. The function of the intrinsic memory trace of the fractional order controller in dampening oscillation in a model of Parkinson's disease. **A**) Two simulations with $\alpha = 1.5$, $\beta = 0.5$, and $K_i = 5788$ in both of them and $K_d = 2.55$ t (black) in one and $K_d = 3.55$ in the other (gray). The symbols are to mark events described in the other panels. **B**) Comparison of the memory trace of the integral and the derivative components for the cases described in A. **C**) Phase plane of the first 100 ms between the memory trace of the derivative and STN activity. **D**) Complete phase plane between the memory trace of the derivative and STN activity.

case, $K_D = 2.55$, the system was under control, and in the other, $K_D = 3.35$, the system oscillated, Fig. 4A. Plotting the memory trace for the integral and derivative elements of the controller show, as expected, that the integral parts track the slow-moving dynamics, while the derivative follows fast changes, Fig. 4B. In the case of the fractional derivative, the response to the onset of the Parkinson's condition causes the memory trace to increase, which then provides a negative feedback into the dynamics, thus reducing the firing rate of the STN. However, the difference between the controlled and oscillatory simulations is that in the oscillatory the larger K_D causes an over-compensation of the memory trace when the firing rate is recovering to the target value, this then results in a larger oscillation than in the controlled case (• in Fig. 4A and B). This can also be seen in the phase plane plots of each case, Fig. 4C and D. For the controlled case, the oscillation is captured by the attractor which slowly moves to the target value. However, in the oscillatory case, the system is not captured by the attractor and escapes from the target value. This dynamic is very similar to our previously reported modeling studies of the effects of fractional order dynamics in the generation of trains of action potentials in neurons [75]. In summary, these analyses show that the $PID^{\alpha>1}_{\beta<1}$ controller is several folds more robust to settings in the gains than the $PID^{\alpha=1}_{\beta=1}$ case.

After showing that the $PID^{\alpha>1}_{\beta<1}$ increases the range of the controller gains we tested the robustness in dampening oscillations when varying the synaptic parameters of the network model. In the network model, the oscillatory behavior arises due to increases in the synaptic weights between GP→STN (ω_{gs}), STN→GP (ω_{sg}), and GP→GP (ω_{gg}). Changes in the other synaptic parameters did not result in oscillatory behavior. In order to explore the synaptic parameters space, we generated 760 combinations of the three synaptic weights randomly distributed from 0 to 200% of the disease state values (Table 2). We ran the 760 simulations for each combination of the fractional orders of the integral, $\alpha = (1,\ 1.3,\ 1.5,\ 1.7)$, and derivative $\beta = (0.3, 0.5\ ,\ 0.7,\ 1)$. Each simulation consisted in running the model 2.5 s with the healthy set of synapses and then another 2.5 s with the disease state. As before, we determined the simulations that were controlled for each conditions of fractional order controllers. This analysis shows that the values of ω_{gs} and ω_{sg} determine whether the simulation was under control (Fig. 5A). The value of ω_{gg} did not contribute to the control of the simulation, except for the cases in which the self-inhibition was so strong that it shut down the activity of the GP (not shown). Since this is not physiologically realistic, those simulations were discarded. In the case of $PID^{\alpha=1}_{\beta=1}$ the fraction of simulations that converged was 0.57, in contrast, for $PID^{\alpha=1.3}_{\beta=0.5}$ this increased to 0.82. In fact, an analysis of the entire data set shows that the maximum robustness to changes in synaptic weights is achieved with $\alpha = 1.3$ and $\beta = [0.5,\ 1]$. After $\alpha \geq 1.7$ the simulations do not converge (Fig. 5B). This analysis shows that fractional order controllers can expand the robustness in controlling the onset of oscillations due to changes in network dynamics with a fixed set of gains.

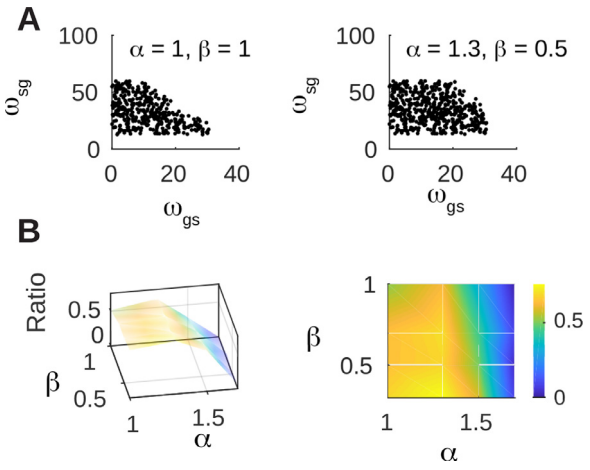

Fig. 5. Fractional order properties in a PID controller increase robustness to changes in synaptic weights. **A**) *Left*, Scatter plot of simulations, out of 760, that were controlled by the classical controller, $PID^{\alpha=1}_{\beta=1}$. Each simulation had a random value of the synaptic weights (ω_{gs}, ω_{sg}, ω_{gg}), up to 200% from the values that caused Parkinson's oscillations. The values of ω_{gg} are not shown because they did not show a correlation with the outcome of the simulations. *Right*, scatter plot of running the same 760 simulations with different orders in the fractional controller, $PID^{\alpha=1.3}_{\beta=0.5}$. **B**) *Left*, Surface plot of the ratio of the simulations that were controlled for each combination of fractional order in the controller, integral, $\alpha = (1,\ 1.3,\ 1.5,\ 1.7)$ for the integral $\beta = (0.3, 0.5\ ,\ 0.7,\ 1)$ for the derivative. *Right*, two-dimensional projection of the data on the left.

7. Discussion

In this paper, we presented a mathematical and modeling study to test the advantages of using fractional order controllers in DBS. Our main result is that the robustness of the controller to changes in the gains of the $PID^{\alpha>1}_{\beta<1}$ are multi-fold to those determined in the classical controller, $PID^{\alpha=1}_{\beta=1}$. Similarly, when fixing the gains of the controller the $PID^{\alpha>1}_{\beta<1}$ was able to control oscillations to a larger range of changes in the synaptic parameters. The general properties of fractional integration and differentiation provide a mixture of information about the monitored biomarker signal (the pathological oscillations) not possible with classical integer value integration or differentiation.

There is increasing interest in using closed-loop DBS for Parkinson's disease. Recent reports show that closed-loop therapies are more effective than open-loop approaches [13,14,21–24,31,37,45–47,63,78]. The challenges are to develop adaptive algorithms that can detect a biomarker and effectively dampen the oscillatory activity. Monitoring tremors or difficulty in moving is not a good predictor of pathological oscillations; instead, the signals within the basal ganglia are monitored, in particular using LFP in the GP. Our model used the delayed synaptic input coming from the STN into the GP as a measure of the LFP. However, depending on the level of biological detail used in the models this measurement could have different characteristics. Our model used firing rates; however, it seems to be possible to trigger closed-loop signals using isolated action potentials. In any case, the use of flexible algorithms is a challenge to implement these devices. There are different strategies, such as linear feedback control, genetic algorithms, and other heuristic processes [15,18,22,61,66,80]. Our approach was different because instead of focusing on continuously modifying the gains of the PID controller we used fractional order components, which intrinsically have the mathematical framework to process non-linear systems. The advantage is that our $PID^{\alpha>1}_{\beta<1}$ can control the onset of Parkinson's oscillations over a wide range of synaptic parameters, suggesting that such a system could handle the physiological changes expected during chronic therapy.

While much work has been done in studying the properties of fractional order controllers, the implementation of such systems has technical hurdles. Computationally, these algorithms are demanding. A fractional order integral or derivative requires taking into account all previous history; thus increasing the computational demand over time. This could be restricted by defining a rolling window over which the two functions are calculated. Another approach, and probably the most important for DBS, is to implement the electronic circuits. Fractional differentiation can be achieved by using fractional capacitors [76]. There are efforts to develop fractional capacitors with different materials [1,3,40]. Recently, fractional capacitor emulators have been developed which could be incorporated into PID controllers [76,77]. As these technologies become available, then they will allow implementing low power integrated circuits with the flexibility provided by fractional components.

Declaration of Competing Interest

The authors declare that they have no known competing financial interests or personal relationships that could have appeared to influence the work reported in this paper.

CRediT authorship contribution statement

Antonio Coronel-Escamilla: Investigation, Writing - original draft. **Jose Francisco Gomez-Aguilar:** Supervision. **Ivanka Stamova:** Investigation. **Fidel Santamaria:** Funding acquisition, Supervision, Investigation, Writing - review & editing.

Acknowledgments

This work was supported in part by the National Institutes of Health BRAIN Theories NIMH-NIBIB R01EB026939, and Mexico National Council for Science and Technology (CONACYT).

References

[1] Agambayev A, Patole SP, Farhat M, Elwakil A, Bagci H, Salama KN. Ferroelectric fractional-order capacitors. ChemElectroChem 2017;4(11):2807–13.
[2] Agarwal R, Sarma SV. Restoring the basal ganglia in Parkinson's disease to normal via multi-input phase-shifted deep brain stimulation. In: 2010 annual international conference of the IEEE engineering in medicine and biology society (EMBC); 2010. p. 1539–42.
[3] Ahmad W, El-Khazali R, Elwakil A. Fractional-order Wien-bridge oscillator. Electron Lett 2001;37(18):1110–12.
[4] Azar AT, Serrano FE. Fractional order sliding mode PID controller/observer for continuous nonlinear switched systems with PSO parameter tuning. International conference on advanced machine learning technologies and applications. Springer; 2018.
[5] Babaei N, Salamci MU. Controller design for personalized drug administration in cancer therapy: successive approximation approach. Opt Control Appl Methods 2018;39(2):682–719.
[6] Baleanu D, Diethelm K, Scalas E, Trujillo JJ. Fractional calculus: models and numerical methods. vol. 3. World Scientific; 2012.
[7] Baleanu D, Jajarmi A, Mohammadi H, Rezapour S. A new study on the mathematical modelling of human liver with Caputo–Fabrizio fractional derivative. Chaos Solitons Fractals 2020;134:109705.
[8] Baleanu D, Jajarmi A, Sajjadi SS, Asad JH. The fractional features of a harmonic oscillator with position-dependent mass. Commun Theor Phys 2020;72(5):055002.
[9] Banaś J, O'Regan D. On existence and local attractivity of solutions of a quadratic Volterra integral equation of fractional order. J Math Anal Appl 2008;345(1):573–82.
[10] Bejjani B-P, Damier P, Arnulf I, Thivard L, Bonnet A-M, Dormont D, et al. Transient acute depression induced by high-frequency deep-brain stimulation. N Engl J Med 1999;1999(340):1476–80.
[11] Benabid AL. Deep brain stimulation for Parkinson's disease. Curr. Opin. Neurobiol. 2003;13(6):696–706.
[12] Beuter A, Bélair J, Labrie C. Feedback and delays in neurological diseases: a modeling study using dynamical systems. Bull. Math. Biol. 1993;55(3):525–41.

[13] Beuter A, Lefaucheur J-P, Modolo J. Closed-loop cortical neuromodulation in Parkinson's disease: an alternative to deep brain stimulation? Clin Neurophysiol 2014;125(5):874–85.
[14] Bouthour W, Mégevand P, Donoghue J, Lüscher C, Birbaumer N, Krack P. Biomarkers for closed-loop deep brain stimulation in Parkinson disease and beyond. Nat Rev Neurol 2019;15(6):343–52.
[15] Brocker DT, Swan BD, So RQ, Turner DA, Gross RE, Grill WM. Optimized temporal pattern of brain stimulation designed by computational evolution. Sci Transl Med 2017;9(371).
[16] Carron R, Chaillet A, Filipchuk A, Pasillas-Lépine W, Hammond C. Closing the loop of deep brain stimulation. Front Syst Neurosci 2013;7.
[17] Coronel-Escamilla A, Gómez-Aguilar J, Alvarado-Méndez E, Guerrero-Ramírez G, Escobar-Jiménez R. Fractional dynamics of charged particles in magnetic fields. Int J Mod Phys C 2016;27(08):1650084.
[18] Coronel-Escamilla A, Torres F, Gómez-Aguilar J, Escobar-Jiménez R, Guerrero-Ramírez G. On the trajectory tracking control for an SCARA robot manipulator in a fractional model driven by induction motors with PSO tuning. Multibody Syst Dyn 2018;43(3):257–77.
[19] Dabiri A, Moghaddam BP, Machado JT. Optimal variable-order fractional PID controllers for dynamical systems. J Comput Appl Math 2018;339:40–8.
[20] Debnath L. Recent applications of fractional calculus to science and engineering. Int J Math Math Sci 2003;2003(54):3413–42.
[21] Eitan R, Bergman H, Israel Z. Closed-loop deep brain stimulation for Parkinson's disease. In: Surgery for Parkinson's disease. Springer; 2019. p. 131–49.
[22] Feng X-j, Greenwald B, Rabitz H, Shea-Brown E, Kosut R. Toward closed-loop optimization of deep brain stimulation for Parkinson's disease: concepts and lessons from a computational model. J Neural Eng 2007;4(2):L14.
[23] Fleming JE, Dunn E, Lowery MM. Simulation of closed-loop deep brain stimulation control schemes for suppression of pathological beta oscillations in Parkinson's disease. Front Neurosci 2020;14 166-166.
[24] Fleming JE, Dunn E, Lowery MM. Simulation of closed-loop deep brain stimulation control schemes for suppression of pathological beta oscillations in Parkinson's disease. Front Neurosci 2020;14.
[25] Follett KA, Weaver FM, Stern M, Hur K, Harris CL, Luo P, et al., and others Pallidal versus subthalamic deep-brain stimulation for Parkinson's disease. N Engl J Med 2010;362(22):2077–91.
[26] Gheisarnejad M, Faraji B, Esfahani Z, Khooban M-H. A Close loop multi-area brain stimulation control for Parkinson's Patients Rehabilitation. IEEE Sens J 2019.
[27] Goharimanesh M, Lashkaripour A, Abouei Mehrizi A. Fractional order PID controller for diabetes patients. J Comput Appl Mech 2015;46(1):69–76.
[28] Gorzelic P, Schiff S, Sinha A. Model-based rational feedback controller design for closed-loop deep brain stimulation of Parkinson's disease. J Neural Eng 2013;10(2):026016.
[29] Grahn PJ, Mallory GW, Khurram OU, Berry BM, Hachmann JT, Bieber AJ, et al. A neurochemical closed-loop controller for deep brain stimulation: toward individualized smart neuromodulation therapies. Front Neurosci 2014;8(169).
[30] Greenberg BD, Malone DA, Friehs GM, Rezai AR, Kubu CS, Malloy PF, et al. Three-year outcomes in deep brain stimulation for highly resistant obsessive–compulsive disorder. Neuropsychopharmacology 2006;31(11):2384–93.
[31] Haddock A, Velisar A, Herron J, Bronte-Stewart H, Chizeck HJ. Model predictive control of deep brain stimulation for Parkinsonian tremor. 2017 8th International IEEE/EMBS Conference on Neural Engineering (NER). IEEE; 2017.
[32] Hale JK, Lunel SMV, Verduyn LS, Lunel SMV. Introduction to functional differential equations. vol. 99. Springer Science & Business Media; 1993.
[33] Holgado AJN, Terry JR, Bogacz R. Conditions for the generation of beta oscillations in the subthalamic nucleus-globus pallidus network. J Neurosci 2010;30(37):12340–52.
[34] Holgado AJN, Terry JR, Bogacz R. Conditions for the generation of beta oscillations in the subthalamic nucleus–globus pallidus network. J Neurosci 2010;30(37):12340–52.
[35] Hu B, Wang Q. Controlling absence seizures by deep brain stimulus applied on substantia nigra pars reticulata and cortex. Chaos Solitons Fractals 2015;80:13–23.
[36] Jajarmi A, Yusuf A, Baleanu D, Inc M. A new fractional HRSV model and its optimal control: a non-singular operator approach. Physica A 2019:123860.
[37] Johnson LA, Nebeck SD, Muralidharan A, Johnson MD, Baker KB, Vitek JL. Closed-loop deep brain stimulation effects on parkinsonian motor symptoms in a non-human primate–Is beta enough? Brain Stimul 2016;9(6):892–6.
[38] Kilbas AA, Srivastava HM, Trujillo JJ. Theory and applications of fractional differential equations. vol. 204. Elsevier Science Limited; 2006.
[39] Koeller R. Applications of fractional calculus to the theory of viscoelasticity. ASME Trans J Appl Mech 1984;51:299–307.
[40] Krishna MS, Das S, Biswas K, Goswami B. Fabrication of a fractional order capacitor with desired specifications: a study on process identification and characterization. IEEE Trans Electron Devices 2011;58(11):4067–73.
[41] Kumar R, Lozano A, Kim Y, Hutchison W, Sime E, Halket E, et al. Double-blind evaluation of subthalamic nucleus deep brain stimulation in advanced Parkinson's disease. Neurology 1998;51(3):850–5.
[42] Kumar R, Lozano AM, Sime E, Lang AE. Long-term follow-up of thalamic deep brain stimulation for essential and parkinsonian tremor. Neurology 2003;61(11):1601–4.
[43] Laxton AW, Tang-Wai DF, McAndrews MP, Zumsteg D, Wennberg R, Keren R, et al. A phase I trial of deep brain stimulation of memory circuits in Alzheimer's disease. Ann Neurol 2010;68(4):521–34.
[44] Li C, Qian D, Chen Y. On riemann-liouville and caputo derivatives. Discrete Dyn Nat Soc 2011;2011.
[45] Little S, Pogosyan A, Neal S, Zavala B, Zrinzo L, Hariz M, et al., and others Adaptive deep brain stimulation in advanced Parkinson's disease. Ann Neurol 2013;74(3):449–57.
[46] Liu C, Wang J, Deng B, Wei X, Yu H, Li H, et al. Closed-loop control of tremor-predominant parkinsonian state based on parameter estimation. IEEE Trans Neural Syst Rehabil Eng 2016;24(10):1109–21.
[47] Liu C, Wang J, Li H, Lu M, Deng B, Yu H, et al. Closed-loop modulation of the pathological disorders of the basal ganglia network. IEEE Trans Neural Netw Learn Syst 2017;28(2):371–82.
[48] Liu X, Zhang M, Richardson AG, Lucas TH, Van der Spiegel J. Design of a closed-loop, bidirectional brain machine interface system with energy efficient neural feature extraction and PID control. IEEE Trans Biomed Circuits Syst 2016;11(4):729–42.
[49] Mayberg HS, Lozano AM, Voon V, McNeely HE, Seminowicz D, Hamani C, et al. Deep brain stimulation for treatment-resistant depression. Neuron 2005;45(5):651–60.
[50] Moro E, Lozano AM, Pollak P, Agid Y, Rehncrona S, Volkmann J, et al., and others Long-term results of a multicenter study on subthalamic and pallidal stimulation in Parkinson's disease. Mov Disord 2010;25(5):578–86.
[51] Obeso JA, Rodriguez-Oroz MC, Rodriguez M, Lanciego JL, Artieda J, Gonzalo N, et al. Pathophysiology of the basal ganglia in Parkinson's disease. Trends Neurosci. 2000;23:S8–S19.
[52] Parastarfeizabadi M, Kouzani AZ. Advances in closed-loop deep brain stimulation devices. J Neuroeng Rehabil 2017;14(1):79.
[53] Parvinian B, Scully C, Wiyor H, Kumar A, Weininger S. Regulatory considerations for physiological closed-loop controlled medical devices used for automated critical care: food and drug administration workshop discussion topics. Anesth. Analg. 2018;126(6):1916.
[54] Pasillas-Lépine W. Delay-induced oscillations in Wilson and Cowan's model: an analysis of the subthalamo-pallidal feedback loop in healthy and parkinsonian subjects. Biol Cybern 2013;107(3):289–308.
[55] Pasillas-Lépine W, Haidar I, Chaillet A, Panteley E. Closed-loop deep brain stimulation based on firing-rate regulation. In: 2013 6th International IEEE/EMBS Conference on neural engineering (NER); 2013. p. 166–9.
[56] Pavlides A, John Hogan S, Bogacz R. Improved conditions for the generation of beta oscillations in the subthalamic nucleus-globus pallidus network. Eur J Neurosci 2012;36(2):2229–39.
[57] Petras I. Fractional-order nonlinear systems: modeling, analysis and simulation. Springer Science & Business Media; 2011.
[58] Plaha P, Gill SS. Bilateral deep brain stimulation of the pedunculopontine nucleus for Parkinson's disease. Neuroreport 2005;16(17):1883–7.
[59] Podlubny I. Fractional-order systems and PI/sup/spl lambda//D/sup/spl mu//-controllers. IEEE Trans Automat Contr 1999;44(1):208–14.
[60] Podlubny I. Fractional differential equations: an introduction to fractional derivatives, fractional differential equations, to methods of their solution and some of their applications. vol. 198. Academic Press; 1998.
[61] Popovych OV, Lysyansky B, Rosenblum M, Pikovsky A, Tass PA. Pulsatile desynchronizing delayed feedback for closed-loop deep brain stimulation. PLoS ONE 2017;12(3):e0173363.
[62] Pravika M, Jacob J. PID controlled fully automated portable duodopa pump for Parkinson's disease patients. Biomed Signal Process Control 2019;50:178–87.
[63] Rosin B, Slovik M, Mitelman R, Rivlin-Etzion M, Haber SN, Israel Z, et al. Closed-loop deep brain stimulation is superior in ameliorating Parkinsonism. Neuron 2011;72(2):370–84.
[64] Rubin JE, Terman D. High frequency stimulation of the subthalamic nucleus eliminates pathological thalamic rhythmicity in a computational model. J Comput Neurosci 2004;16(3):211–35.
[65] Sabatier J, Lanusse P, Melchior P, Oustaloup A. Fractional order differentiation and robust control design. Intell Syst Control Autom 2015;77:13–18.
[66] Santaniello S, Fiengo G, Glielmo L, Grill WM. Closed-loop control of deep brain stimulation: a simulation study. IEEE Trans Neural Syst Rehabil Eng 2011;19(1):15–24.
[67] Sharifi N, Ozgoli S, Ramezani A. Multiple model predictive control for optimal drug administration of mixed immunotherapy and chemotherapy of tumours. Comput Methods Programs Biomed 2017;144:13–19.
[68] Sharma R, Deepak K, Gaur P, Joshi D. An optimal interval type-2 fuzzy logic control based closed-loop drug administration to regulate the mean arterial blood pressure. Comput Methods Programs Biomed 2020;185:105167.
[69] Soltan A, Xia L, Jackson A, Chester G, Degenaar P. Fractional order PID system for suppressing epileptic activities. 2018 IEEE International Conference on Applied System Invention (ICASI). IEEE; 2018.
[70] Stamova I. Mittag-Leffler stability of impulsive differential equations of fractional order. Q Appl Math 2015;73(3):525–35.
[71] Stamova I. On the Lyapunov theory for functional differential equations of fractional order. Proc Am Math Soc 2016;144(4):1581–93.
[72] Stamova I, Stamov G. Functional and impulsive differential equations of fractional order: qualitative analysis and applications. CRC Press; 2017.
[73] Su F, Wang J, Deng B, Wei X-L, Chen Y-Y, Liu C, et al. Adaptive control of Parkinson's state based on a nonlinear computational model with unknown parameters. Int J Neural Syst 2015;25(01):1450030.
[74] Tan N, Atherton DP, Yüce A. Computing step and impulse responses of closed loop fractional order time delay control systems using frequency response data. Int J Dyn Control 2017;5(1):30–9.

[75] Teka W, Stockton D, Santamaria F. Power-law dynamics of membrane conductances increase spiking diversity in a hodgkin-huxley model. PLoS Comput. Biol. 2016;12(3):e1004776.
[76] Tsirimokou G, Psychalinos C, Elwakil A, Salama K. Experimental verification of on-chip CMOS fractional-order capacitor emulators. Electron Lett 2016;52(15):1298–300.
[77] Tsirimokou G, Psychalinos C, Freeborn TJ, Elwakil AS. Emulation of current excited fractional-order capacitors and inductors using OTA topologies. Microelectronics J 2016;55:70–81.
[78] Velisar A, Syrkin-Nikolau J, Blumenfeld Z, Trager M, Afzal M, Prabhakar V, et al. Dual threshold neural closed loop deep brain stimulation in Parkinson disease patients. Brain Stimul 2019;12(4):868–76.
[79] Weinberg SH, Santamaria F. History dependent neuronal activity modeled with fractional order dynamics. Computational models of brain and behavior; 2017. p. 531–48.
[80] Wilson C, Beverlin B, Netoff T. Chaotic Desynchronization as the Therapeutic Mechanism of Deep Brain Stimulation. Front Syst Neurosci 2011;5(50).
[81] Yıldız TA, Jajarmi A, Yıldız B, Baleanu D. New aspects of time fractional optimal control problems within operators with nonsingular kernel. Discret Contin Dyn Syst-S 2020;13(3):407–28.